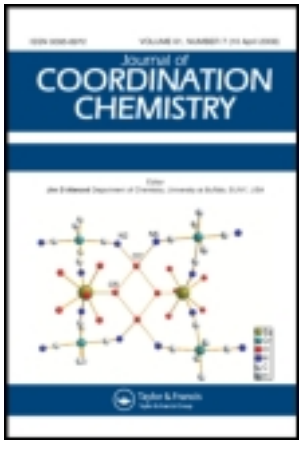

Journal of Coordination Chemistry
Publication details, including instructions for authors and subscription information:
http://www.tandfonline.com/loi/gcoo20

Synthesis, characterization, and biological activity of some lanthanide ternary complexes

Zhihui Shen [a b], Dongfang Xu [a], Ningning Cheng [a], Xianan Zhou [a], Xiaoke Chen [a], Yinghao Xu [a] & Qizhuang He [a]

[a] Key Laboratory of Resource Chemistry of Ministry of Education, College of Life and Environmental Science, Shanghai Normal University, No. 100 Guilin Road, Shanghai 200234, P.R. China

[b] Huangyan Middle School, Zhejiang 318020, P.R. China

Published online: 06 Jul 2011.

To cite this article: Zhihui Shen, Dongfang Xu, Ningning Cheng, Xianan Zhou, Xiaoke Chen, Yinghao Xu & Qizhuang He (2011) Synthesis, characterization, and biological activity of some lanthanide ternary complexes, Journal of Coordination Chemistry, 64:13, 2342-2352, DOI: 10.1080/00958972.2011.595482

To link to this article: http://dx.doi.org/10.1080/00958972.2011.595482

Journal of Coordination Chemistry
Vol. 64, No. 13, 10 July 2011, 2342–2352

Synthesis, characterization, and biological activity of some lanthanide ternary complexes

ZHIHUI SHEN†‡, DONGFANG XU*†, NINGNING CHENG†, XIANAN ZHOU†, XIAOKE CHEN†, YINGHAO XU† and QIZHUANG HE*†

†Key Laboratory of Resource Chemistry of Ministry of Education, College of Life and Environmental Science, Shanghai Normal University, No. 100 Guilin Road, Shanghai 200234, P.R. China
‡Huangyan Middle School, Zhejiang 318020, P.R. China

(*Received 25 November 2010; in final form 9 May 2011*)

Five complexes have been synthesized by the reaction of lanthanide(III) nitrate with 2-thenoyltrifluoroacetone (HTTA) and *p*-hydroxybenzoic acid (L). The complexes have been characterized by elemental analysis, molar conductivity, FT-IR, UV-Vis, ^{1}H NMR, TG-DTA, XPS, and transmission electron microscope. The general formula of the complexes is $Na[Ln(TTA)_3L]$ ($Ln = La^{3+}, Ce^{3+}, Nd^{3+}, Eu^{3+}, Er^{3+}$). The antibacterial activities indicate that all five complexes exhibit antibacterial ability against *Escherichia coli* and *Staphylococcus aureus* with broad antimicrobial spectrums. The antitumor activity of the five complexes against K562 tumor cell *in vitro* is measured using methyl thiazolyl tetrazolium (MTT) colorimetry. The results show that the complexes induce K562 tumor cell apoptosis, and the complexes exhibit inhibitory effect on leukemia K562 cells.

Keywords: Lanthanide complex; Antibacterial; Antitumor

1. Introduction

Considerable attention has been paid to lanthanide complexes [1–6]. Lanthanides have good physical and chemical properties as well as anti-inflammation, antitumor, and antithrombogenic properties because of their electron configuration [7, 8]. Some lanthanide complexes are biological probes for medical diagnoses and drug development [9]. Recently, some studies showed that lanthanide complexes might have a potential role in the treatment of tumor cell lines [10] and the different coordination modes of drugs toward metal ions have received more attention [11]. Trifluoromethylated compounds have received considerable attention, with diverse applications in materials science, agrochemistry, and biomedical chemistry due to their chemical, physical, and biological properties [12]; β-diketones can form complexes with almost every metal and metalloid [13]. 2-Thenoyltrifluoroacetone (HTTA) is a β-diketone and Acheampong's [14] studies showed that it has biological activity. HTTA was an inhibitor of the mitochondrial electron flux [15, 16], and mitochondria

*Corresponding authors. Email: xdf26@shnu.edu.cn; hqz@shnu.edu.cn

Journal of Coordination Chemistry
ISSN 0095-8972 print/ISSN 1029-0389 online © 2011 Taylor & Francis
DOI: 10.1080/00958972.2011.595482

play an important role in the mechanisms of cytotoxicity and antitumor activity of complexes [17]. Several metal complexes of HTTA have been synthesized, characterized, and evaluated as luminescent probes [18]. However, studies on biological activities of the lanthanide complexes with 2-thenoyltrifluoroacetone (HTTA) and *p*-hydroxybenzoic acid (L) have not been reported. The selection of *p*-hydroxybenzoic acid (L) as the second ligand in the complexes may increase the biocompatibility of these complexes [19].

Due to the importance of lanthanide complexes and our interest in the synthesis of lanthanide complexes [1, 8, 20, 21], we report herein the synthesis, characterization, and biological activities of lanthanide complexes with HTTA and *p*-hydroxybenzoic acid (L), in continuation of our research to develop new antitumor and antibacterial agents which may provide basis for application in biological activities for lanthanide complexes [20].

2. Experimental

2.1. *Materials and measurements*

RPMI 1640 and tetrazolium salt 3-(4,5-dimethylthiazol-2-yl)-2,5-diphenyltetrazolium bromide (MTT) were purchased from Sigma; fetal calf serum (FCS) was purchased from GiBCo, No. 1165723; sodium dodecylsulfate (SDS) was purchased from Sino-American Biotechnology; $Ln(NO_3)_3 \cdot 6H_2O$ was purchased from the National Medicines Group Shanghai Chemical Reagent Co., Ltd. All reagents were of analytical grade and used without purification.

Elemental analyses were determined on an Elementar Vario EL III elemental analyzer. The infrared (IR) spectra were measured at room temperature on a PK-60000 FT-IR using KBr pellets from 4000 to 400 cm^{-1}. UV spectra were recorded on a Perkin-Elmer17. ^1H NMR spectra were measured using a Varian VXR 300 MHz NMR spectrometer. TG-DTA curves were recorded on a thermal Oflex DTA derivatograph at 10 K min^{-1} with the samples heated in the atmosphere by a Perkin-Elmer Pyris Diamond. The transmission electron microscope (TEM) image was recorded on a JEM-1200EX TEM. XPS was recorded on a PHI 5000 Versa probe.

2.2. *Bacteria and cells*

Staphylococcus aureus (*S. aureus ATCC6358P*) and *Escherichia coli* (*E. coli ATCC11229*) were provided by Shanghai Drug Institute, Chinese Academy of Sciences; cell strain: human leukemia K562 cells were obtained from the Cell Bank of the Chinese Academy of Sciences (Shanghai, China).

2.3. *Synthesis of Na[Ln(TTA)$_3$L]*

2-Thenoyltrifluoroacetone (1.33 g, 6 mmol) was dissolved in 30 mL of ethanol. NaOH (1 N, 6 mL) and a solution of $Ln(NO_3)_3 \cdot 6H_2O$ (2 mmol) in 10 mL of water was added. The mixture was heated to 60°C with stirring. After 1 h, 2 mmol *p*-hydroxybenzoic acid and NaOH with a molar ratio of 1 : 1 in ethanol was added dropwise under stirring and

the solution was heated to 60°C for 4 h [22]. The solvent was removed by rotary evaporation. Excess unbonded complex was washed away with water three times and dried *in vacuo*.

2.4. *Biological assay*

2.4.1. *In vitro* evaluation of antibacterial activity. (a) *Method of paper disc diffusion*. $0.005\,mol\,L^{-1}$ aqueous solution of $Ln(NO_3)_3 \cdot 6H_2O$, *p*-hydroxybenzoic acid, $Na[Ln(TTA)_3L]$, and $0.015\,mol\,L^{-1}$ HTTA were prepared using DMSO as solvent, and the antibacterial activity of all the compounds against *S. aureus* and *E. coli* were studied. The bacterium suspension concentration was controlled as 5×10^5–$5 \times 10^6\,cfu\,mL^{-1}$; diameters of filter paper were 5 mm, and for the experiments, flat plates were incubated at 37°C (bacterium) for 18–24 h [21]. Their inhibition diameter (including filter paper) was measured with a vernier caliper.

(b) *Method of nutrient broth dilution*. Nutrient broth was employed for bacterial growth. The tested $Ln(NO_3)_3 \cdot 6H_2O$, 2-thenoyltrifluoroacetone (HTTA), *p*-hydroxybenzoic acid (L), and $Na[Ln(TTA)_3\,L]$ were prepared in nutrient broth medium and diluted in concentrations from 50 to $800\,\mu g\,mL^{-1}$. Inocula containing $1 \times 10^6\,cfu\,mL^{-1}$ were obtained from broth cultures [21]. The lowest concentration ($\mu g\,mL^{-1}$) of compounds, which inhibited the growth of bacteria after 24 h incubation at 37°C, was taken as the minimum inhibitory concentration (MIC). All the experiments were repeated three times and the results were expressed in average values.

2.4.2. Test of antitumor activity. Antitumor activities of the new compound on leukemia K562 cells were tested using the MTT method. Briefly, $1 \times 10^5\,mL^{-1}$ leukemia K562 cells and each compound at various concentrations were put into 1 mL medium and then added to each well of a 96-well plate. Tests at each concentration were conducted in eight holes. The plate was incubated at 37°C in a humidified atmosphere containing 5% CO_2 for 44 h. 10 μL of MTT solution was then added to each well. After the plate was further incubated for 4 h, 100 μL of 10% SDS was added to each well to solubilize formazan dye. The optical density (OD) at 570 nm was read by an enzyme-linked immunosorbent assay (ELISA) reader the next day [1, 21]. The mean and standard deviation of each group were calculated.

$$\text{The inhibition rate (IR, \%)} = (1 - OD_{complex}/OD_{blank}) \times 100\%.$$

2.4.3. Morphological observation of apoptosis. Morphological observation of the new compounds induced apoptosis of leukemia K562 cells after staining with acridine orange (AO, 10%) was carried out on a fluorescence microscope; 30 μL of the treated leukemia K562 cells were collected and stained with 10 μL of AO. When the AO entered the cells, the DNA exhibited a green fluorescence and the RNA exhibited orange fluorescence. Fifteen minutes later, control cells and apoptosis were observed on a fluorescent microscope and photographed. Morphological observations revealed

Table 1. Elemental analysis and molar conductance data of complexes.

Complexes	Found (Calcd) %			χ_m ($S\,cm^2\,mol^{-1}$)
	RE	C	H	
$Na[La(TTA)_3L]$	14.30(14.45)	38.51(38.67)	1.53(1.77)	84
$Na[Ce(TTA)_3L]$	14.45(14.54)	38.48(38.62)	1.84(1.76)	83
$Na[Nd(TTA)_3L]$	15.15(14.91)	38.65(38.46)	1.64(1.75)	89
$Na[Eu(TTA)_3L]$	15.45(15.58)	38.36(38.15)	1.81(1.74)	85
$Na[Er(TTA)_3L]$	17.02(16.89)	37.40(37.56)	1.79(1.72)	87

Numbers in parentheses are the stoichiometry (%) results of the complex.

typical apoptotic features in the infected cells, including cell shrinkage and rounding, chromosome condensation, and formation of apoptotic body-like vesicles [23].

3. Results and discussion

3.1. *Elemental analysis*

The Ln(III) percentage was determined by complexometric titration with EDTA, according to the method described by He [1]. Analytical data of Ln(III), C, H, and N percentages (found/calculated) for the complexes are listed in table 1. The analytical data are consistent with the calculated values of general formulae of the Ln(III) complexes. The molar conductance measurements of the complexes were performed in ethanol (with a concentration of $1 \times 10^{-3}\,mol\,L^{-1}$) at room temperature. The values varied between 83 and $89\,S\,cm^2\,mol^{-1}$, indicating that they are electrolytes in ethanol [24]. Elemental analysis and molar conductivity of the complexes are presented in table 1.

3.2. *FT-IR*

Table 2 shows the IR spectral data of the ligands and lanthanide ternary complexes. IR spectra of the five complexes are similar, but different from those of the two ligands. IR spectra of HTTA showed $\nu_{s\ C=O}$ at 1662 and $1645\,cm^{-1}$, which shifted to lower energy ($1612–1620\,cm^{-1}$) in the complexes, indicating that C=O is coordinated to Ln(III). New bands at $550–560\,cm^{-1}$ ($\nu_{Ln–O}$) further supported the formation of Ln–O [25]. Bands at 1405 and $1544\,cm^{-1}$ are attributed to the stretching vibrations of $\nu_{s\ COO–}$ and $\nu_{as\ COO–}$ of L, which shift to 1407–1411 and $1537–1541\,cm^{-1}$, respectively, showing coordination. According to Deacon and Philips [26] and Taylor *et al.* [27], if the separation ($\Delta = \nu_{as} - \nu_s$) in lanthanide carboxylates is lower than that in the carboxylate, the coordination of carboxylate with lanthanide is mainly bidentate chelating, bidentate bridging, or tridentate chelating-bridging. The separation values ($\Delta = \nu_{as} - \nu_s$) between $\nu_{as\ COO}$ and $\nu_{s\ COO}$ is $130\,cm^{-1}$ in the complexes, lower than that in L ($139\,cm^{-1}$), which shows that the carboxylate is bidentate chelating with lanthanide. These results show that both HTTA and L are coordinated to lanthanide.

Table 2. IR spectral data of ligands and complexes.

	HTTA	L		
Ligands and complexes	ν_s C=O	ν_s COO^-	ν_{as} COO^-	νLn–O
Ligand	1654	1405	1544	–
Na[La(TTA)$_3$L]	1613	1409	1540	556
Na[Ce(TTA)$_3$L]	1612	1407	1538	550
Na[Nd(TTA)$_3$L]	1620	1410	1539	558
Na[Eu(TTA)$_3$L]	1615	1408	1541	563
Na[Er(TTA)$_3$L]	1619	1411	1537	560

Table 3. ^{1}H NMR spectra of ligand and La complex in $CDCl_3$ (ppm).

Complex	δCH=CH	δCH=CH	δCH=CH	δCH=CH	δCOOH	δOH	δCH_2
L	6.94	7.96			11.05	5.2	
HTTA	6.98	7.76	7.84	–		14.52	
La complex	6.22	7.13	7.79	8.05	–	5.6	2.52

3.3. *UV-Vis spectra*

Supplementary material shows UV-Vis spectra of ligands and complexes measured at 1×10^{-4} mol L^{-1} using DMSO. The ε_{max} of the complexes are different from that of the free ligands, indicating the formation of new complexes.

UV spectra of the five complexes are similar, but different from those of the two ligands. HTTA shows a main absorption at 287 nm for $\pi \rightarrow \pi^*$ transition, shifted to higher energy and a new band at about 338–341 nm can be observed in the complexes. L shows one strong peak at 245 nm that shifted to 258–262 nm in the complexes. The other peak at 207 nm appears at approximately the same frequency as observed in the complexes (205–206 nm), indicating that –OH is uncoordinated [28]. Both C=O of HTTA and COO^- of L are involved in metal complexation.

3.4. *^{1}H NMR*

^{1}H NMR spectra of *p*-hydroxybenzoic acid (L), HTTA, and La complex were performed in $CDCl_3$ and the chemical shifts in ppm are: *p*-hydroxybenzoic acid (L): $\delta = 6.94$ ppm (s, 2H, Ar–H), $\delta = 7.96$ ppm (s, 2H, Ar–H), $\delta = 11.05$ ppm (s, 1H, COOH), $\delta = 5.$ 20 ppm (s, 1H, OH), and HTTA: $\delta = 6.98$ ppm (s, 1H, thiophene–H), $\delta = 7.76$ ppm (s, 1H, thiophene–H), $\delta = 7.84$ ppm (s, 1H, thiophene–H), $\delta = 4.17$ ppm (s, 2H, CH_2) (table 3).

Comparison between L and the complex found that ^{1}H NMR signals of complex are in the same places as free ligands with decreasing intensity. In the complex, resonances of *p*-hydroxybenzoic acid (6.94, 7.96) shift 0.09 and 0.29 downfield compared to free L (7.23, 8.05). The proton resonance of carboxyl disappeared.

Table 4. XPS of ligands and complexes.

	RE		O		O
HTTA	–	–	–	–	532.08
L	–	–	531.40	533.68	–
$La(NO)_3 \cdot 6H_2O$	839.71	856.52	–	–	–
$Ce(NO)_3 \cdot 6H_2O$	850.63	886.32	–	–	–
$Nd(NO)_3 \cdot 6H_2O$	983.90	1006.81	–	–	–
$Eu(NO)_3 \cdot 6H_2O$	890.45	945.15	–	–	–
$Er(NO)_3 \cdot 6H_2O$	978.81	1013.79	–	–	–
$Na[La(TTA)_3L]$	837.12	855.21	531.51	534.20	532.70
$Na[Ce(TTA)_3L]$	849.95	886.52	531.55	534.32	532.75
$Na[Nd(TTA)_3L]$	982.80	1006.11	531.97	534.88	532.90
$Na[Eu(TTA)_3L]$	889.54	943.36	531.89	534.72	532.81
$Na[Er(TTA)_3L]$	976.51	1011.85	531.85	534.80	532.86

Free HTTA exists in $CDCl_3$ solutions 100% in the enol form, displaying a prominent enol proton resonance at 14.52. In complexes, this resonance disappears while a methine signal at 2.52 appeared, indicating coordination of HTTA to La(III). Signals of the thienyl protons in complex (6.22, 7.13, and 7.79) shifted 0.76, 0.63, and 0.05 upfield compared to those of free HTTA (6.98, 7.76, and 7.84). The ^1H NMR signals of the complex are in the same places as free ligand with increasing intensity.

3.5. *TG-DTA*

TG-DTA curves of the five ternary complexes are similar when heated in air from 25°C to 1000°C. The weight loss of these complexes exhibited good agreement with the stoichiometry. The endothermic peak of framework rupture of complexes is at 216–221°C (Supplementary material). Decomposition of these complexes is through two stages with the second decomposition to the oxide, accompanied by a strong exothermic effect with one peak. The complexes decomposed completely at 560°C with residues of lanthanide oxide and sodium oxide. TG-DTA results showed no weight loss in the TG curve around 25–110°C, suggesting that the complex does not contain crystal water [28]. This is consistent with the molecular formula.

3.6. *XPS*

Data of the photoelectron spectroscopy of ligands and complexes are shown in table 4. The binding energy of oxygens in HTTA and L were less than that of oxygens in complexes. Because the oxygens of ligands are coordinated, the electron cloud density was reduced resulting in higher binding energy. The binding energy of oxygen in HTTA was 532.08 eV. In contrast, the binding energy of oxygen in $Na[La(TTA)_3L]$, $Na[Ce(TTA)_3L]$, $Na[Nd(TTA)_3L]$, $Na[Eu(TTA)_3L]$, and $Na[Er(TTA)_3L]$ were 532.70, 532.75, 532.90, 532.81, and 532.86 eV. The binding energies of oxygen in L were at 531.40 and 533.68 eV, while in $Na[La(TTA)_3L]$, $Na[Ce(TTA)_3L]$, $Na[Nd(TTA)_3L]$, $Na[Eu(TTA)_3L]$, and $Na[Er(TTA)_3L]$ they were (531.51, 534.20), (531.55, 534.32), (531.97, 534.88), (531.89, 534.72), and (531.85, 534.80) eV. The binding energy of Ln ions in the complexes decreased because of increased electron cloud density, suggesting

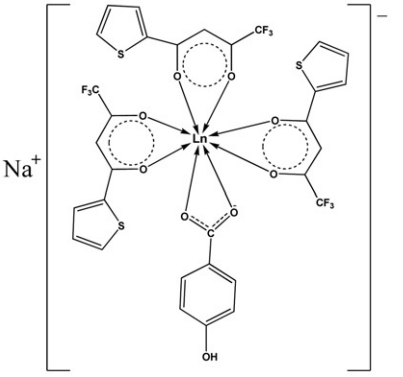

Scheme 1. The proposed structure of $Na[Ln(TTA)_3L]$.

that Ln ions are electron acceptors. The binding energies of Ln ions in $La(NO_3)_3 \cdot 6H_2O$, $Ce(NO_3)_3 \cdot 6H_2O$, $Nd(NO_3)_3 \cdot 6H_2O$, $Eu(NO_3)_3 \cdot 6H_2O$, and $Er(NO_3)_3 \cdot 6H_2O$ were (839.71, 856.52), (850.63, 886.32), (983.90, 1006.81), (890.45, 945.15), and (978.81, 1013.79) eV. In contrast, the binding energies of Ln ions in $Na[La(TTA)_3L]$, $Na[Ce(TTA)_3L]$, $Na[Nd(TTA)_3L]$, $Na[Eu(TTA)_3L]$, and $Na[Er(TTA)_3L]$ were (837.12, 855.21), (849.95, 886.52), (982.80, 1006.11), (889.54, 943.36), and (976.51, 1011.85) eV. Data in table 4 shows that oxygens in HTTA and L are coordinated to lanthanide.

3.7. *TEM*

The morphology and grain size of the complexes were investigated by TEM (Supplementary material). The complex presents a rod-like shape, and the grain size is about 50 nm which is consistent with calculated results by the Scherrer equation; thus the grain size reaches nano-class size. Dispersion of particles is good. The complex possesses small size effect, less side-effect, and less dosage because of its nanostructure, laying a foundation for their biological activity. The TEM studies of the complex made it possible to conclude that the complex nanoparticles have very well-defined rod-like shapes, which can easily penetrate the membrane of the cells and react with the cells. So the complex may have good biological activity.

Based on the above studies, a tentative coordination structure for the complex is proposed (scheme 1).

3.8. *Antibacterial activity*

The antibacterial activities of the complexes, $LnNO_3$ and the ligands are evaluated using the paper disc diffusion method and the nutrient broth dilution method against *E. coli ATCC11229* and *S. aureus ATCC6358P*. Penicillin (North China Pharmaceutical Co. Ltd, D0211107, Hebei 050015, China) was used as standard drug for bacteria, with diameter of growth inhibition of 17 and 56 mm against *E. coli* and *S. aureus*, respectively. The MIC of Penicillin was 150 and 1.6 $\mu g\,mL^{-1}$ against *E. coli* and *S. aureus*, respectively (not presented in table 5).

Table 5. Antibacterial *in vitro* activity expressed as diameter of growth inhibition area and MIC.

Complex	Diameter of growth inhibition area (mm)			MIC ($\mu g\,mL^{-1}$)	
	Concentration ($mol\,L^{-1}$)	*E. coli*	*S. aureus*	*E. coli*	*S. aureus*
HTTA	0.015	13	12	>400	>400
L	0.005	7	6	>600	>600
$La(NO)_3 \cdot 6H_2O$	0.005	8	7	>500	>500
$Ce(NO)_3 \cdot 6H_2O$	0.005	9	7	>500	>500
$Nd(NO)_3 \cdot 6H_2O$	0.005	7	9	>500	>500
$Eu(NO)_3 \cdot 6H_2O$	0.005	8	9	>500	>500
$Er(NO)_3 \cdot 6H_2O$	0.005	9	7	>500	>500
$Na[La(TTA)_3L]$	0.005	21	22	130	110
$Na[Ce(TTA)_3L]$	0.005	20	21	160	130
$Na[Nd(TTA)_3L]$	0.005	21	23	130	110
$Na[Eu(TTA)_3L]$	0.005	20	21	150	130
$Na[Er(TTA)_3L]$	0.005	22	23	100	120

The antibacterial activity results as diameter of growth inhibition area (mm) and the MIC ($\mu g\,mL^{-1}$) are listed in table 5. All the tested lanthanide ternary complexes exhibit antibacterial activities against *E. coli* and *S. aureus*, better than each free ligand. The Er complex shows relatively favorable antibacterial activity with diameter of growth inhibition area (22 mm, 23 mm) and the MIC (100 $\mu g\,mL^{-1}$, 120 $\mu g\,mL^{-1}$) against *E. coli* and *S. aureus*. So the antimicrobial spectrum of the complexes is broad.

Increasing in antibacterial activity of the complex may be due to the effect of complexation, which considerably reduces the polarity of the metal ion because of partial sharing of its positive charge with the donor groups. π-Electron delocalization in the chelating ring also increases the lipophilic nature of the central metal atom, which inclines to permeation through the lipid layers of the cell membrane [29–31]. The antibacterial mechanism is presumably that microbial cell membrane is damaged, which leads to intracellular protein denaturation and inhibits activity of cell respiration enzymes and electron-transport enzymes.

3.9. *Test of antitumor activity*

Antitumor activities of the complexes were determined by MTT reduction assay against K562 cells. Their proliferation inhibitory effect was compared to the ligand. When K562 cells were exposed to 0.05–0.15 $\mu g\,mL^{-1}$ of complexes for 48 h, a dose-dependent growth inhibition effect was observed (table 6). IC_{50} (50% inhibiting concentration) values are derived and ($n = 3$) presented in table 7. The lanthanide and the ligands promote proliferation of cancer cells. The complexes ($\geq 0.05\,\mu g\,mL^{-1}$) inhibited proliferation of cancer cells, with inhibitory rates of 18.9%, 15.0%, 19.5%, 21%, and 25%, respectively. At 0.1–0.15 $\mu g\,mL^{-1}$, the inhibitory rate was up to 50% (except Ce complex). The IC_{50} values (La complex, Nd complex, Eu complex, Er complex) were 0.1, 0.12, 0.14, and 0.1 $\mu g\,mL^{-1}$, respectively. At 0.15 $\mu g\,mL^{-1}$, the inhibitory rate of Ce complex was 38.5%. Anticancer activities of complexes are superior to each ligand and the ligands promote cell growth in the same concentrations of the complexes.

Table 6. Inhibiting percentage of K562 tumor cell growth cycle detected by MTT reduction assay.

	Control (%)				
	Concentration ($\mu g\,mL^{-1}$)				
	0.050	0.075	0.100	0.125	0.150
$La(NO)_3 \cdot 6H_2O$	−38.0	−48.2	−40.9	−35.4	−33.8
$Ce(NO)_3 \cdot 6H_2O$	−36.1	−41.3	−36.7	−35.0	−30.2
$Nd(NO)_3 \cdot 6H_2O$	−29.2	−26.4	−23.8	−20.2	−16.3
$Eu(NO)_3 \cdot 6H_2O$	−37.0	−36.2	−30.1	−26.7	−23.9
$Er(NO)_3 \cdot 6H_2O$	−41.4	−51.0	−43.2	−34.8	−27.9
HTTA	−24.0	−36.3	−30.9	−39.8	−37.0
L	−30.1	−35.3	−46.8	−42.0	−21.2
$Na[La(TTA)_3L]$	18.9	31.0	54.1	61.8	69.0
$Na[Ce(TTA)_3L]$	15.0	19.2	25.1	32.9	38.5
$Na[Nd(TTA)_3L]$	19.5	29.3	48.0	55.6	58.4
$Na[Eu(TTA)_3L]$	21.0	23.2	45.6	51.2	54.6
$Na[Er(TTA)_3L]$	25.0	36.2	53.6	60.0	68.5

(−): Promote proliferation of cancer cells; (+): inhibit proliferation of cancer cells.

Table 7. IC_{50} values of the complexes.

Complex	$Na[La(TTA)_3L$	$Na[Nd(TTA)_3L]$	$Na[Eu(TTA)_3L]$	$Na[Er(TTA)_3L]$
IC_{50} value ($\mu g\,mL^{-1}$)	0.1	0.12	0.14	0.1

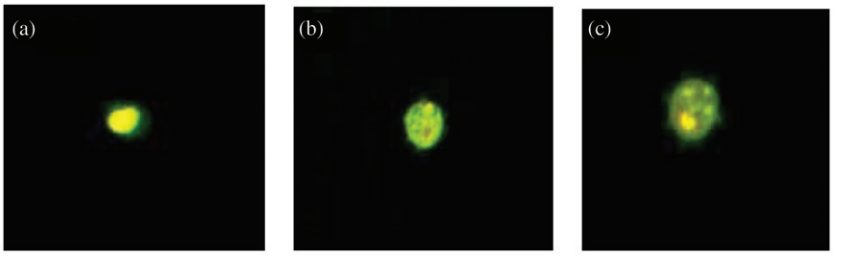

Figure 1. Morphological observations revealed in the infected cells: (a) normal cell, (b) karyorrhexis, and (c) apoptotic body-like vesicles.

Table 7 shows that IC_{50} values of the complexes varied between 0.1 and $0.15\,\mu g\,mL^{-1}$; when $IC_{50} < 10\,\mu g\,mL^{-1}$, the drug was thought to have anticancer activity [32]. So the complexes have antitumor properties [33].

The antitumor activities may be due to the extended planar structure caused by conjugation from the chelation of the rare ion with the ligands [34]. The antitumor mechanism is presumably that complexes incorporate in K562 cells and interact with DNA, which changes the protein expression, inhibiting mitosis of cancer cells.

The morphological observation of apoptosis of La complex is shown in figure 1. Fifteen minutes later, the control cells and the apoptosis are observed on a

fluorescent microscope. We can probably conclude that the La complex can induce apoptosis of leukemia K562 cells.

4. Conclusion

Synthesis and characterization of five lanthanide complexes with antibacterial and antitumor activities have been achieved. The antibacterial activities show that the complexes have better antibacterial ability against *E. coli* and *S. aureus* than the free ligands. The La complex shows the most favorable antibacterial activity. The complexes exhibit inhibitory effect on the leukemia K562 cells. Some studies have revealed that some lanthanide complexes are potent cytotoxic agents [10]. The IC_{50} values of the four complexes were 0.1, 0.12, 0.14, and 0.1 $\mu g\,mL^{-1}$, respectively; the La and Er complexes show the most favorable antitumor activity.

Acknowledgments

We are grateful to the National Nature Science Foundation of China (20671063, 20973114), Key Laboratory of Resource Chemistry of Ministry of Education, Shanghai Leading Academic Discipline Project (S30406), Shanghai Key Laboratory of Rare Earth Functional Materials (07dz22303), Key Subject of Shanghai Normal University (DZL806), and the research of Shanghai Normal University (No. SK201048) for the financial support.

References

[1] D.F. Xu, S.Z. Ma, Q.Z. He, G.Y. Du. *J. Rare Earths*, **26**, 643 (2008).
[2] B. Yan, Y.S. Song, Z.X. Chen. *Mol. Struct.*, **694**, 115 (2004).
[3] S.V. Eliseevaa, J.-C.G. Bünzli. *Chem. Soc. Rev.*, **39**, 189 (2010).
[4] E.J. Werner, A. Datta, C.J. Jocher, K.N. Raymond. *Angew. Chem., Int. Ed.*, **47**, 8568 (2008).
[5] P. Hermann, J. Kotek, V. Kubicek, I. Lukes. *Dalton Trans.*, 3027 (2008).
[6] M. Woods, D.E. Woessner, A.D. Sherry. *Chem. Soc. Rev.*, **35**, 500 (2006).
[7] J.Z. Ni. *Bioinorganic Chemistry of Rare Earth*, p. 288, Science Press, Beijing (2002).
[8] H. Yu, Q.Z. He, J. Yang, W.J. Zheng. *J. Rare Earths*, **24**, 4 (2006).
[9] A.-L. Gassner, C. Duhot, J.-C.G. Bünzli, A.-S. Chauvin. *Inorg. Chem.*, **47**, 7802 (2008).
[10] I. Kostova, T. Stefanova. *J. Coord. Chem.*, **62**, 3187 (2009).
[11] N.E.A. El-Gamel. *J. Coord. Chem.*, **62**, 2239 (2009).
[12] G. Blay, I. Fernández, A. Monleón, J.R. Pedro, C. Vila. *Org. Lett.*, **11**, 441 (2009).
[13] J. Annaraj, S. Srinivasan, K.M. Ponvel. *J. Inorg. Biochem.*, **99**, 669 (2005).
[14] Y.B. Acheampong, A.A. Adimado, K.S. Patel. *Indian J. Pharm. Sci.*, **46**, 207 (1984).
[15] Y. Dong, S.J. Berners-Price, D.R. Thorburn, T. Antalis, J. Dickinson, T. Hurst, L. Qiu, S.K. Khoo, P.G. Parsons. *Biochem. Pharmacol.*, **53**, 1673 (1997).
[16] M.P. Rigobello, L. Messori, G. Marcon, M.A. Cinellu, M. Bragadin, A. Folda, G. Scutari, A. Bindoli. *J. Inorg. Biochem.*, **98**, 1634 (2004).
[17] M.J. McKeage, L. Maharaj, S.J. Berners-Price. *Coord. Chem. Rev.*, **232**, 127 (2002).
[18] C.Y. Peng, H.J. Zhang, J.B. Yu. *J. Phys. Chem. B*, **109**, 15278 (2005).
[19] G.J. Xu, Y.Y. Kou, L. Feng, S.P. Yan, D.Z. Liao, Z.H. Jiang, P. Cheng. *Appl. Organomet. Chem.*, **20**, 351 (2006).
[20] D.F. Xu, Y.M. Xu, N.N. Chen, X.A. Zhou, Y. Shi, Q.Z. He. *J. Coord. Chem.*, **63**, 2360 (2010).

[21] M.F. Zhou, Q.Z. He. *J. Rare Earths*, **26**, 473 (2008).
[22] P. Lenaerts, K. Driesen, R.V. Deun, K. Binnemans. *Chem. Mater.*, **17**, 2148 (2005).
[23] L. Calcarifer, J. Fish. *Diseases*, **31**, 825 (2008).
[24] W.J. Geary. *Coord. Chem. Rev.*, **7**, 81 (1971).
[25] J. Chen, H.X. Xu, H. Du. *J. Chin. Rare Earth Soc.*, **26**, 239 (2008).
[26] G.B. Deacon, R.J. Philips. *Coord. Chem. Rev.*, **33**, 227 (1980).
[27] M.D. Taylor, C.P. Carte, C.I. Wynter. *Inorg. Nucl. Chem.*, **30**, 1503 (1968).
[28] Y.M. Song, J.P. Xu, L. Ding, Q. Hou, J.W. Liu, Z.L. Zhu. *J. Inorg. Biochem.*, **103**, 396 (2009).
[29] Y.L. Song, Y.T. Li, Z.Y. Wu. *J. Inorg. Biochem.*, **102**, 1691 (2008).
[30] T. Ahamad, N. Nishat, S. Parveen. *J. Coord. Chem.*, **61**, 1963 (2008).
[31] B.A. Song, S. Yang, Y.P. Hong, G.P. Zhang, L.H. Jin, D.Y. Hu. *J. Fluorine Chem.*, **126**, 1419 (2005).
[32] P.R. Twentyman, N.E. Fox, J.K. Rees. *Br. J. Haematol.*, **71**, 19 (1989).
[33] X.L. Wang, H. Chao. *J. Inorg. Biochem.*, **98**, 423 (2004).
[34] M. Jiang, Y.T. Li, Z.Y. Wu, Z.Q. Liu, C.W. Yan. *J. Inorg. Biochem.*, **103**, 833 (2009).